Published in final edited form as:
Mol Microbiol. 2010 October ; 78(1): 138–157. doi:10.1111/j.1365-2958.2010.07317.x.

Proteobactin and a yersiniabactin-related siderophore mediate iron acquisition in *Proteus mirabilis*

Stephanie D. Himpsl[1], **Melanie M. Pearson**[1], **Carl J. Arewång**[1,2], **Tyler D. Nusca**[1,2], **David H. Sherman**[1,2], and **Harry L. T. Mobley**[1,*]

[1] Department of Microbiology and Immunology, University of Michigan Medical School, Ann Arbor, Michigan 48109

[2] Life Sciences Institute and Departments of Medicinal Chemistry and Chemistry, University of Michigan, 210 Washtenaw Avenue, Ann Arbor, MI 48109

Abstract

Proteus mirabilis causes complicated urinary tract infections (UTI). While the urinary tract is an iron-limiting environment, iron acquisition remains poorly characterized for this uropathogen. Microarray analysis of *P. mirabilis* HI4320 cultured under iron limitation identified 45 significantly up-regulated genes ($P \leq 0.05$) that represent 21 putative iron-regulated systems. Two gene clusters, PMI0229-0239 and PMI2596–2605, encode putative siderophore systems. PMI0229-0239 encodes a nonribosomal peptide synthetase (NRPS)-independent siderophore (NIS) system for producing a novel siderophore, proteobactin. PMI2596-2605 are contained within the high-pathogenicity island, originally described in *Yersinia pestis*, and encodes proteins with apparent homology and organization to those involved in yersiniabactin production and uptake. Cross-feeding and biochemical analysis shows that *P. mirabilis* is unable to utilize or produce yersiniabactin, suggesting that this yersiniabactin-related locus is functionally distinct. Only disruption of both systems resulted in an *in vitro* iron-chelating defect; demonstrating production and iron-chelating activity for both siderophores. These findings clearly show that proteobactin and the yersiniabactin-related siderophore function as iron acquisition systems. Despite the activity of both siderophores, only mutants lacking the yersiniabactin-related siderophore reduce fitness *in vivo*. The fitness requirement for the yersiniabactin-related siderophore during UTI shows, for the first time, the importance of siderophore production *in vivo* for *P. mirabilis*.

Keywords

Proteus; uropathogenesis; iron acquisition; ferri-siderophore

Introduction

Iron, an essential element, is required for the function of many proteins and enzymes involved in diverse biological processes including oxygen transport, gene regulation, and nitrogen fixation. Under aerobic conditions and neutral pH, iron exists in the insoluble ferric (Fe^{3+}) form, which can be toxic following interaction with oxygen and oxygen-reduced species. During colonization of the host, pathogens must overcome host iron sequestration to establish infections because free iron is essentially unavailable *in vivo*. To counterbalance

*Corresponding author: Mailing address: Department of Microbiology and Immunology, University of Michigan Medical School, 5641 Medical Science Building II, 1150 West Medical Center Drive, Ann Arbor, MI 48109. Phone: (734) 763-3531. Fax: (734) 764-3562. hmobley@umich.edu.

iron-limiting conditions and maintain iron homeostasis, bacterial species have evolved various iron transport systems, intracellular iron stores, redox stress resistance systems, and iron responsive regulatory elements to control the expression of genes involved in diverse cellular functions (Andrews *et al.*, 2003).

One way bacteria acquire extracellular ferric iron is by secreting ferric chelators known as siderophores that scavenge iron from the environment during iron-limiting conditions. Over 500 siderophores have been described and can be classified into three groups; catecholates, hydroxamates, and hydroxycarboxylates (Miethke & Marahiel, 2007). Precursors for siderophore biosynthesis include citrate, amino acids, dihydroxybenzoate, and N^5-acyl-N^5-hydroxyornithine (Winkelmann, 2002). Often, genes that encode the biosynthetic enzymes for siderophores are clustered with genes for ferri-siderophore transport (Wandersman & Delepelaire, 2004, Koster, 2001, Crosa & Walsh, 2002). The mechanism of siderophore synthesis and transport is tightly regulated by the ferric uptake regulator (Fur) protein in response to iron availability (Ernst *et al.*, 1978, Crosa & Walsh, 2002, Hantke, 2001).

Once synthesized and transported outside the bacterial cell, the siderophore chelates ferric iron with high affinity. The ferri-siderophore, in turn, binds with high specificity to a TonB-dependent outer membrane receptor in Gram-negative bacterial envelopes. Transport into the cell is driven by cytosolic membrane potential mediated by the energy-transducing TonB-ExbB-ExbD system which requires the direct contact of TonB and the outer membrane receptor (Braun, 1995, Tuckman & Osburne, 1992). Once in the periplasmic space, the ferri-siderophore is shuttled by a periplasmic binding protein to a cytosolic membrane ATP-binding cassette (ABC) transporter. The ferri-siderophore is delivered to the cytosol of the bacterium where iron is reduced to the ferrous (Fe^{2+}) form and dissociates from the siderophore (Neilands, 1995, Faraldo-Gomez & Sansom, 2003, Wandersman & Delepelaire, 2004, Ratledge & Dover, 2000).

Previous reports have indicated that *Proteus mirabilis*, a species within the *Enterobacteriaceae* and an important etiologic agent of complicated urinary tract infection (UTI) (Mobley & Warren, 1987, Warren *et al.*, 1982), lacks detectable siderophore production (Massad *et al.*, 1995, Marcelis *et al.*, 1978, Miles & Khimji, 1975). The Arnow and Csaky tests failed to detect catechol- or hydroxamate-type siderophores, respectively, when testing *P. mirabilis* P18 (Evanylo *et al.*, 1984). These findings were confirmed with gas chromatography in conjunction with mass spectroscopy (Evanylo *et al.*, 1984). However, analysis of the newly annotated *P. mirabilis* HI4320 genome (Pearson *et al.*, 2008) revealed at least two gene clusters with genes related to both siderophore biosynthesis and ABC transport. One of these appears to be a novel nonribosomal peptide synthetase (NRPS)-independent siderophore (NIS) system, herein termed proteobactin that has not been previously described in any bacterial species. The other gene cluster contains the *nrp* operon which has been previously described to be up-regulated during iron limitation in *P. mirabilis* U6450 (Gaisser & Hughes, 1997). Recently, the *nrp* operon has been shown to be encoded within the high-pathogenicity island (HPI) in *P. mirabils* HI4320 that has homology to the HPI of *Yersinia spp*. (Flannery *et al.*, 2009) In addition to the possibility that *nrp* has a function related to iron limitation, the metabolite, α-hydroxyisovaleric acid, has been identified as a possible siderophore (Evanylo *et al.*, 1984). α-keto acids produced by amino acid deaminases and α-hydroxycarboxylic acids have also been postulated as possible siderophores in *Proteus*, *Providencia*, and *Morganella* species (Drechsel *et al.*, 1993, Massad *et al.*, 1995). Despite these studies, none of these metabolites nor those produced by the *nrp* gene products have been shown to possess iron-chelating properties.

Studies on uropathogenic *Escherichia coli* have shown that the urinary tract is iron-limited and that iron acquisition by outer membrane receptors is important during UTI (Alteri &

Mobley, 2007, Torres *et al.*, 2001, Hagan & Mobley, 2009, Snyder *et al.*, 2004). Consistent with this, multiple outer membrane proteins of *P. mirabilis* are up-regulated in both human urine and iron-limiting medium (Shand *et al.*, 1985) and three outer membrane proteins induced by iron-starvation are involved in heme uptake in *P. mirabilis* 6515 (Piccini *et al.*, 1998). One of these, was shown to function as a heme receptor that contributes to the uropathogenesis of *P. mirabilis* 6515 (Lima *et al.*, 2007). Using signature-tagged mutagenesis (STM), we previously identified five genes (PMI3120; putative TonB-dependent receptor, PMI2605; putative 4′-phosphopantetheinyl transferase *nrpG*, PMI2959; putative iron ABC transporter permease, PMI0842; putative TonB-dependent receptor, PMI0030; biopolymer transport protein *exbD*) associated with iron acquisition in *P. mirabilis* HI4320 that when mutated attenuated the bacterium (Burall *et al.*, 2004, Himpsl *et al.*, 2008).

Since iron acquisition remains poorly defined for *P. mirabilis*, we sought to define the global response to iron limitation by first using microarray analysis. This approach allowed for the identification of 21 putative iron acquisition systems based upon the 45 significantly up-regulated genes during *in vitro* iron limitation. Molecular and biochemical characterization of two of these iron acquisition systems verified that these genes are transcriptionally up-regulated during iron limitation, repressed by iron, and are responsible for siderophore production in this human pathogen.

Results

Differential expression of *P. mirabilis* genes during iron limitation

Gene expression of *P. mirabilis* HI4320 cultured under iron limitation was analyzed by microarray. A concentration of 15 μM Desferal, an iron-chelator, inhibited the growth rate of *P. mirabilis* in LB medium (Fig. 1). Microarray analysis of cells cultured in LB medium with and without 15 μM Desferal showed that 1017 genes were differentially expressed: 872 were up-regulated and 145 were down-regulated. Fold-change for all 1017 genes was ≥ 2-fold and calculated based upon the ratio of average spot intensity between these conditions. Of these genes, Significance Analysis of Microarray (SAM) identified 45 significantly up-regulated genes (Table S1) and 43 significantly down-regulated genes (Table S2).

The 45 significantly up-regulated genes represent 21 putative iron acquisition systems. These systems include the energy transducing complex TonB-ExbB-ExbD, genes for heme uptake (PMI0409, PMI1424, and *hmuR1R2STUV*), an aerobic ferrous iron uptake system (*sitABCD*) (Fisher *et al.*, 2009), two putative ferri-siderophore systems (*nrpSUTABG* and PMI0229-0239), and three putative ferri-siderophore transporters (*ireA*, PMI0331, and PMI2957-2960) (Table 1). Other genes induced during iron limitation are a putative iron utilization protein PMI1437, two putative TonB-dependent systems that may be involved in colicin uptake, PMI1551-1548 and PMI0842, and systems with potential iron-sulfur clusters, *sufABCDSE*, *bfd*, and PMI0176-0172. As expected, in contrast to *sitABCD* the *P. mirabilis* ferrous iron uptake system *feoAB* was not up-regulated ≥ 2-fold during aerobic iron limitation. Genes repressed during iron limitation include predicted iron storage proteins and iron-metalloproteins.

To validate the results of the microarray, quantitative RT-PCR (qPCR) was performed on select genes that were iron responsive *in vitro*. A total of six individual up-regulated genes (*exbD*, TonB-dependent receptor PMI0842, *sitA*, *hmuR1*, *glpD*/*glyD*, *bfd*) and one significantly down-regulated gene (*ftnA*) were verified by qPCR (Fig. 2A). As expected, all genes except *glpD*/*glyD* were up-regulated > 2-fold and *ftnA* was down-regulated > 2-fold during culture of *P. mirabilis* HI4320 in 15 μM Desferal (Fig. 2A). Putative siderophore biosynthesis and ABC transport gene clusters encoding the capacity to synthesize the

yersiniabactin-related siderophore, *nrp* (PMI2596-2605) and proteobactin, *pbt* (PMI0229-0239) were also tested by qPCR to verify up-regulation (Fig. 2B, C). Putative siderophore TonB-dependent receptor, PMI2596, and all genes in putative *nrp* operon (PMI2597-2605) were up-regulated > 2-fold (Fig. 2B). Genes of the *pbt* gene cluster (PMI0229-0239) were up-regulated > 2-fold, except *pbtH* (PMI0239) (Fig. 2C). Both *nrp* and *pbt* gene clusters contain consensus sequences for ferric uptake regulator (Fur) binding (Fig. 3) and, consistent with this, the transcription of *pbt* genes are repressed by the addition of 25 μM $FeCl_3{\cdot}6H_2O$ to bacteria cultured in iron-chelated LB medium (Fig 2C). Both of these putative siderophore systems are organized as operons as demonstrated using RT-PCR; the *nrp* system consists of two transcripts and the *pbt* system is transcribed in three units (Fig. 3).

Since the urinary tract is iron-limited (Alteri & Mobley, 2007, Hagan & Mobley, 2009, Torres *et al.*, 2001, Snyder *et al.*, 2004) and the *nrp* and *pbt* operons are induced during iron limitation *in vitro*, the expression of one putative siderophore biosynthesis gene from each of the two systems was examined *in vivo*. We assessed the transcription of these genes during infection by comparing expression of *pbtA* (PMI0232) and *nrpR* (PMI2599) using qPCR to quantify RNA purified from wild-type *P. mirabilis* cultured in LB medium and from *P. mirabilis* recovered from the urine of infected mice. Bacteria recovered from urine of infected mice up-regulated both siderophore synthetase genes *in vivo* as compared to LB medium. Interestingly, *pbtA* appeared to display a greater level of induction than *nrpR* under these conditions ($P = 0.0002$) (Fig. 2D).

Characterization of the yersiniabactin-related locus in *P. mirabilis*

Previously, we have shown that the *nrp* genes (PMI2597-2605) are located on a pathogenicity island in *P. mirabilis* HI4320 (Flannery *et al.*, 2009). These genes have homology to genes required for synthesis of yersiniabactin, a nonribosomal peptide synthetase (NRPS) siderophore, which is encoded on the high-pathogenicity island (HPI) of *Yersinia spp*. (Flannery *et al.*, 2009, Carniel *et al.*, 1996). In *P. mirabilis*, the putative yersiniabactin receptor, PMI2596, is annotated as a TonB-dependent receptor and shares 27% amino acid sequence identity with the yersiniabactin/pesticin receptor gene *psn* (Fig. 4A, Table 2). Genes PMI2597-2605 are divergently transcribed from PMI2596 (Fig. 3) and make up an operon encoding a major facilitator superfamily (MFS) transporter, a conserved hypothetical protein, two putative nonribosomal peptide synthases including *nrpS*, two putative siderophore biosynthesis genes *nrpU* and *nrpT*, two putative siderophore ABC transport ATP-binding/permeases *nrpA* and *nrpB*, and putative 4′-phosphopantetheinyl transferase *nrpG* (Fig. 4A). To maintain consistency with the current nomenclature, the three previously uncharacterized genes that are expressed in this operon are designated *nrpX* (PMI2597), *nrpY* (PMI2598), and *nrpR* (PMI2599).

Despite the homology to yersiniabactin biosynthesis and transport genes in other *Enterobacteriaceae* (Table 2), the yersiniabactin-related siderophore synthesized by *P. mirabilis* HI4320 is predicted to lack modification by salicylate. Genes involved in salicylic acid biosynthesis and incorporation, *pchB*, *pchA*, and *irp5* in *Pseudomonas syringae* pv. tomato DC3000 and *ybtE* and *ybtS* in *Y. pestis* KIM that are essential for yersiniabactin function in these bacteria are absent in the *P. mirabilis nrp* locus (Fig. 4A). The *P. mirabilis nrp* operon also lacks a linked transcriptional regulator analogous to PSPTO2606 and YbtA (Fig. 4A). Another distinctive product of the *P. mirabilis nrp* operon is the presence of a conserved hypothetical protein encoded by *nrpY* (PMI2598), which has similarity to methyl-transferases found in NRPS systems (Fig. 4A). Additionally, the 4′-phosphopantetheinyl-transferase located at the end of the *P. mirabilis nrp* operon, *nrpG*, is encoded separately from the yersiniabactin operon on the *Y. pestis* chromosome (*ybtD*) (Fig. 4A). Likewise, the

4′-phosphopantetheinyl-transferase of *P. syringae* is absent from the yersiniabactin operon (Fig. 4A).

P. mirabilis is unable to grow on LB agar containing 25 μM Desferal. However, in cross-feeding assays, *P. mirabilis* growth is restored (Fig. 5A, Table 3) by uropathogenic *E. coli* (UPEC) strain 536 that produces both enterobactin and yersiniabactin (Brzuszkiewicz *et al.*, 2006). This restoration of *P. mirabilis* growth was abolished when cross-fed by a UPEC 536 construct that lacks both enterobactin and yersiniabactin (Fig. 5C,Table 3). Unexpectedly, *P. mirabilis* was incapable of growth on iron chelator when cross-fed by the 536 strain that produces yersiniabactin and lacks only enterobactin (Fig. 5B,Table 3). In addition, UPEC CFT073, a strain incapable of synthesizing yersiniabactin (Bultreys *et al.*, 2006), can also restore the growth defect in *P. mirabilis* in cross-feeding assays (Fig. 5D, Table 3); in this assay, *P. mirabilis* swarms around *E. coli* CFT073. This ability of *P. mirabilis* to utilize enterobactin is independent of both the *nrp* and *pbt* iron acquisition systems (Table 3). These surprising findings show that yersiniabactin is not able to be utilized by *P. mirabilis* and suggests that despite the clear evolutionary relationship, the *nrp* locus is not involved in the production and uptake of yersiniabactin *per se*.

The lack of yersiniabactin production is also supported by an HPLC analysis showing the absence of UV absorbance maxima (310 and 385 nm) characteristic of yersiniabactin (Jones *et al*., 2007) when concentrated supernatants from *P. mirabilis* cultured under iron limitation were analyzed by HPLC and compared directly to concentrated supernatants of *E. coli* 536 mutants *entF::kan* and *entF ybtS::kan* (Fig. 6). Furthermore, extracts of the same experimental *P. mirabilis* HI4320 and control *E. coli* 536 cultures were prepared using previously reported methods (Bultreys *et al*., 2006, Jones *et al*., 2007) and analyzed by ESI-LC-MS. Monitoring in positive ion mode, *m/z* matching that of a ferri-yersiniabactin species described by Jones and colleagues (2007) could be detected in *E. coli* 536 *entF::kan* (expected: 535.1, observed: 534.8); the same signal could not be detected from *E. coli entF ybtS::kan* negative control or *P. mirabilis* HI4320 samples (Fig. 6). These data support the assertion that *P. mirabilis nrp*, while highly similar to the yersiniabactin operon of other species, is incapable of producing a molecule identical to yersiniabactin.

Identification of a novel NRPS-independent siderophore system that synthesizes proteobactin

The second siderophore biosynthesis operon of *P. mirabilis* HI4320 encodes a novel NRPS-independent siderophore (NIS) pathway that is predicted to produce a hydroxycarboxylate siderophore. The first two genes, PMI0229-0230, are predicted to encode an ABC transport permease protein and an ABC transport ATP-binding subunit, are expressed as a two gene transcript (Fig. 3C, D). *PbtI* (PMI0231) encodes a putative citrate lyase β subunit and is transcribed as a single mRNA from the opposite coding strand (Fig. 3C, D). Citrate lyase β activity converts citric acid to oxaloacetate, which is a key biosynthetic precursor and could be the preferred substrate of the putative siderophore biosynthesis protein encoded by *pbtA* (PMI0232). Because oxaloacetate is a closely related metabolic intermediate to α-ketoglutarate, a well known substrate for NIS type B synthetases (Challis, 2005), it is probable that *pbtA* also belongs to the type B subfamily of NIS synthetases. The polycistron that contains the putative NIS synthetase also codes for a putative TonB-dependent siderophore receptor, a putative lysine/ornithine decarboxylase, a putative pyridoxal-phosphate dependent enzyme, a putative octopine/opine/tauropine dehydrogenase, a MFS-family transporter, a substrate-binding protein, and a hypothetical protein (Fig. 3C, D).

All known NIS biosynthetic pathways utilize at least one siderophore synthetase with homology to hydroxamate synthesis enzymes IucA (NIS type A) and IucC (NIS type C) (Challis, 2005). In line with this, the siderophore synthetase from this operon in *P. mirabilis*

has 21% and 25% identity to IucA and IucC of uropathogenic *E. coli*, respectively. Upon further examination, the closest homolog to this *P. mirabilis* hydroxamate synthetase is found in an uncharacterized siderophore system of the phytopathogens *Pectobacterium* (formerly *Erwinia*) *carotovora* subsp. *atroseptica* and *P. carotovora* subsp. *carotovora* (54% identity to both). The primary siderophore biosynthetic enzyme used by these systems and the *P. mirabilis* synthetase encoded by PbtA have only 27–28 % identity to the achromobactin biosynthetic enzyme AcsD, which has recently been classified as the prototype member of a new family of enzymes, NIS type B, that synthesize a hydroxycarboxylate NIS in *P. chrysanthemi* (Munzinger *et al.*, 2000, Franza *et al.*, 2005, Schmelz *et al.*, 2009).

To determine which NIS synthetase subfamily the synthetase of proteobactin represents, 92 protein sequences homologous to siderophore synthetase PbtA, identified by BLASTP, were aligned using Clustal W (Thompson *et al.*, 1994) and used for phylogenetic analysis of the related NIS enzymes (Fig. 7). The resulting phylogeny clearly identified the three known NIS subfamilies as distinct clades and placed PbtA within the same clade as Y4xN (Fig. 7), a siderophore synthetase of *Sinorhizobium fredii* described to be a type B NIS synthetase (Challis, 2005). This phylogenetic analysis suggests that the NIS of *P. mirabilis* is a type B NIS synthetase and the genes that encode for the capacity to produce this NIS, proteobactin, are referred to as *pbtABCDEFGHI*, for proteobactin synthesis (Fig. 4B).

Siderophore production by *P. mirabilis* HI4320

To detect siderophore production by both the yersiniabactin-related and proteobactin systems, we examined *P. mirabilis* on CAS agar and by the CAS assay. Following growth of HI4320 on CAS agar, a color change of CAS from blue to orange, indicating iron chelation, was observed as a halo surrounding the bacteria. This effect was less pronounced than that caused by uropathogenic *E. coli* CFT073 (Fig. 8A). The iron chelation effect produced by wild-type HI4320 on CAS agar is similar to that of either proteobactin (*pbtA*) or yersiniabactin-related (*nrpR*) biosynthesis mutants (Fig. 8A). However, a double mutant in both siderophore systems (*nrpR pbtA*) is unable to chelate iron from the dye (Fig. 8A). This iron-chelating defect in the double mutant is similar to *E. coli* CFT073 *entF::kan iucB::cam*, which does not produce siderophores (Torres *et al.*, 2001) (Fig. 8A).

To quantify the observed iron-binding properties of both *P. mirabilis* proteobactin and the yersiniabactin-related siderophore, a soluble CAS assay was performed using 50-fold concentrated *P. mirabilis* supernatants from log-phase cells cultured in MOPS defined medium (Neidhardt *et al.*, 1974) with and without 0.1 mM $FeCl_3{\cdot}6H_2O$. Results of this quantitative CAS assay clearly demonstrate that when cultured under iron limitation, *P. mirabilis* produces and releases one or more molecules that chelate iron from the ferri-CAS complex ($P = 0.0001$) (Fig. 8B). This same result was seen for each *P. mirabilis* single siderophore biosynthesis mutant; presence of either proteobactin or the yersiniabactin-related siderophore was sufficient to chelate iron during iron limitation (indicated by a decrease in A_{630}) ($P < 0.0001$) (Fig. 8B). In contrast, significant iron-chelation by the *P. mirabilis* double siderophore biosynthesis mutant was not observed during iron limitation (Fig. 8B). This is consistent with the iron-chelating defect seen with the *E. coli* CFT073 enterobactin/aerobactin double siderophore mutant *entF::kan iucB::cam*. Interestingly, iron chelation by either single synthetase mutant was modestly increased as compared to wild-type HI4320 ($P < 0.0001$) (Fig. 8B). Despite our best efforts to standardize bacterial cultures by optical density, it is possible that variation and siderophore stability during sample preparation could be responsible for this result. qPCR analysis determined this phenotype is not due to the up-regulation of one synthetase gene in the absence of the other synthetase gene (data not shown).

To determine whether the yersiniabactin-related siderophore and proteobactin are common in other *P. mirabilis* isolates, ten urine isolates and ten non-UTI isolates were screened by PCR for the presence of siderophore biosynthesis genes *pbtA* and *nrpR*. As expected, 100% (10/10) of the *P. mirabilis* urine isolates contain both *pbtA* and *nrpR* while only 50% (5/10) of the *P. mirabilis* non-UTI isolates contain both genes. Therefore, urine isolates are more likely to have both *pbtA* and *nrpR*, ($P = 0.0325$) compared to *P. mirabilis* non-UTI isolates.

In vivo contribution of siderophore systems during ascending UTI

To determine the role of siderophores during murine ascending UTI, siderophore synthetase and TonB-dependent receptor mutants of proteobactin or the yersiniabactin-related siderophore were transurethrally inoculated into the bladders of CBA/J mice in independent and cochallenge competition experiments with wild-type HI4320. In independent infections, the loss of the proteobactin siderophore system alone or a double mutant in both siderophore synthetase genes did not attenuate HI4320 (Table 4). During independent infection, the yersiniabactin-related synthetase/receptor mutant (Nrp^{SR}) appeared to colonize better than wild-type HI4320 ($P < 0.05$) (Table 4) where the median CFU/g was less than one-half log greater for Nrp^{SR} than HI4320 (Fig. S2). In cochallenge competition experiments, the strain lacking only proteobactin did not have a fitness defect and loss of Pbt^{SR} may slightly increase fitness in the kidneys ($P = 0.034$) (Table 5). Interestingly, the yersiniabactin-related synthetase/receptor mutant (Nrp^{SR}) was significantly out-competed by wild-type in the bladder ($P = 0.004$) and kidneys ($P = 0.027$) (Table 5). Similarly, the yersinibactin-related synthetase and proteobactin synthetase/receptor mutant ($Nrp^{S}Pbt^{SR}$) was significantly out-competed by wild-type in the bladder ($P = 0.019$) (Table 5). These data, from both independent and cochallenge infections, consistently indicate that the yersiniabactin-related siderophore had a greater contribution for *P. mirabilis* fitness *in vivo*.

Discussion

It is well known that the urinary tract is iron-limited. Despite this, little is known about iron acquisition by the common uropathogen *P. mirabilis*. To improve our understanding of iron acquisition and identify potential siderophore systems utilized by this pathogen; we examined the genome-wide transcriptome from bacteria cultured under iron-replete and iron-deficient conditions. As expected, many genes predicted to encode iron acquisition systems or proteins were up-regulated during iron limitation including *exbD* and three additional genes that have been previously identified by our signature-tagged mutagenesis (STM) screens (Burall *et al.*, 2004, Himpsl *et al.*, 2008). The iron acquisition systems identified in the present study are grouped into functional classes that include genes required for heme uptake, aerobic ferrous iron uptake (Fisher *et al.*, 2009), ferric citrate transport, and siderophore biosynthesis and transport. These microarray findings may not comprehensively demonstrate expression of every iron acquisition system employed by *P. mirabilis* HI4320; however, this study has been useful to propose a model of iron acquisition and transport strategies utilized by this human pathogen (Fig. 9).

Numerous unsuccessful attempts to detect siderophores in *P. mirabilis* have led to speculation that *P. mirabilis* is a poor siderophore producer (Marcelis *et al.*, 1978, Massad *et al.*, 1995, Miles & Khimji, 1975, Evanylo *et al.*, 1984). However the results of the microarray indicated the up-regulation of a number of genes related to siderophore synthesis during iron limitation including a known and unknown amino acid deaminase *aad* and PMI2149 both of which could possibly chelate iron (Drechsel *et al.*, 1993, Massad *et al.*, 1995). Also, genes homologous to the transport and metabolism of ferri-siderophores, such as putative ABC substrate-binding protein PMI0331, ABC transport system PMI2957-2960, putative iron utilization protein PMI1437, and putative esterase PMI2503 were up-regulated during iron limitation. A total of four putative TonB-dependent ferri-siderophore receptors

were up-regulated during iron limitation: *ireA*, PMI0363, PMI2596, and PMI0233. Two of these ferri-siderophore receptors, PMI0233 and PMI2596, are located in regions that encode for both siderophore biosynthesis and ABC transport, which is a common feature of known ferri-siderophore systems (Wandersman & Delepelaire, 2004, Koster, 2001, Crosa & Walsh, 2002).

One of these *P. mirabilis* siderophore systems encodes the *nrp* operon and is closely related to the synthesis, uptake, and ABC transport of yersiniabactin, a nonribosomal peptide synthetase (NRPS) siderophore encoded on the HPI of *Yersinia spp*. (Flannery *et al.*, 2009). Despite apparent homology and organization to yersiniabactin, cross-feeding assays indicate that *P. mirabilis* is unable to utilize yersiniabactin produced by UPEC strain 536 (Table 3, Fig. 5). This finding suggests that the *nrp* locus of *P. mirabilis* is functionally distinct from yersiniabactin. Indeed, the *nrp* synthesis and ABC transport genes of *P. mirabilis* differ equally from the known yersiniabactin synthesis and ABC transport genes of *Y. pestis* KIM, *E. coli* 536, *P. syringae* pv. tomato DC3000, and *Photorhabdus luminescens* TT01 (Table 2). Previously, three yersiniabactin loci evolutionary groups have been described in *Y. pestis*, *P. syringae*, and *P. luminescens* (Bultreys et al., 2006). The *nrp* locus of *P. mirabilis* may likely encode a fourth yersiniabactin evolutionary group. Interestingly, the genes for salicylic acid biosynthesis and incorporation required for yersiniabactin synthesis in these *Enterobacteriaceae* are absent from the *P. mirabilis nrp* operon. Despite the absence of these genes, we have shown that the *nrp* system of *P. mirabilis* is able to chelate iron suggesting the salicylic acid biosynthesis genes may be located elsewhere on the chromosome or perhaps the *nrp* locus has evolved to synthesize a novel yersiniabactin-related siderophore that does not require this modification. Furthermore, efforts to chemically detect yersiniabactin from *P. mirabilis* were unsuccessful (Fig. 6), supporting the possibility of an evolutionary divergence from producing traditional yersiniabactin.

In addition to the *nrp*/yersiniabactin-related system, *P. mirabilis* also has a previously uncharacterized NRPS-independent siderophore (NIS) system. This newly identified NIS system, proteobactin, has similarity to NIS group A (IucA) and NIS group C (IucC) synthetases. Closer scrutiny reveals the proteobactin synthetase, PbtA, is most closely related to a predicted synthetase that is part of an uncharacterized siderophore system found in the phytopathogens, *Pectobacterium carotovora* subsp. *atroseptica* and subsp. *carotovora*. Proteobactin and the molecules produced by these putative systems are distinct from achromobactin, a recently identified NIS system in *P. chrysanthemi* (Franza *et al.*, 2005, Munzinger *et al.*, 2000, Schmelz *et al.*, 2009). Furthermore, both these subspecies of *P. carotovora* and *P. mirabilis* do not possess the *acs* genes required for achromobactin synthesis suggesting proteobactin represent a new NIS system (Franza *et al.*, 2005). Phylogenetic analysis (Fig. 7) places PbtA among the type B subfamily clade of NIS synthetases. Other genes in the NIS operon potentially involved in the synthesis of proteobactin include *pbtD* and *pbtE*. PbtD is a putative pyridoxal-phosphate dependent enzyme and PbtE is a putative octopine/opine/tauropine dehydrogenase. The pyridoxal-phosphate dependent enzyme could be responsible for the incorporation or tailoring of thiol-containing moieties into the proteobactin hydroxycarboxylate siderophore (Kessler, 2006). The octopine/opine/tauropine dehydrogenase could be involved in modification of the primary amine of a siderophore precursor by condensing it to an enzymatically-reduced pyruvate or similar small ketone. This may function in incorporating an additional chelating carboxylate to siderophore biosynthesis intermediates (Mihara *et al.*, 2005). Future biochemical studies will be useful to discern the molecular basis and biochemical function for the NIS genes and enzymes (Oves-Costales *et al.*, 2009).

Initial studies verified that proteobactin and the *nrp* genes were up-regulated during *in vitro* iron limitation of *P. mirablis* HI4320. Likewise, proteobactin and the yersiniabactin-related

siderophore biosynthesis genes *pbtA* and *nrpR* were up-regulated following experimental urinary tract infection of mice with HI4320, not only validating our *in vitro* findings but supporting prior evidence that the urinary tract is an iron-limiting environment and confirming that both siderophores are expressed *in vivo.* Interestingly, *P. mirabilis* urine isolates were significantly more likely to have both *pbtA* and *nrpR*, ($P = 0.0325$) compared to *P. mirabilis* non-UTI isolates. This finding suggests that both siderophore systems are significantly more prevalent in *P. mirabilis* strains that infect the urinary tract than those that colonize other body sites.

The universal chemical assay to detect siderophore production independent of structure (Schwyn & Neilands, 1987) clearly shows that the yersiniabactin-related siderophore and proteobactin of *P. mirabilis* HI4320 chelate iron *in vitro* (Fig. 8). However, we speculate that iron chelation in this assay is inefficient compared to other species, such as *E. coli* CFT073. Unlike the robust conversion from blue to orange observed for *E. coli*, *P. mirabilis* generates a less intense, but nevertheless significant, color change from blue to orange on CAS agar (Fig. 8A). Similarly, in quantitative liquid CAS assays, comparable levels of siderophore activity to *E. coli* CFT073 could only be detected when supernatant from *P. mirabilis* was concentrated 50-fold. A mutant with defects in both proteobactin and yersiniabactin-related biosynthesis (but not single mutants) abolished iron-chelation, suggesting that both systems are producing functional molecules that chelate iron *in vitro* (Fig. 8A, B). Additional experiments determined that this phenotype was not due to a growth defect, as inactivation of both siderophore synthesis systems did not affect the *in vitro* growth of *P. mirabilis* in LB medium alone or in LB medium with 15 μM Desferal (Fig. S1). During growth, the presence of other iron transport systems as identified by microarray could compensate for the loss of one or both siderophore biosynthesis systems (Table 1).

It is likely that the compensatory action of other iron acquisition and uptake systems in *P. mirabilis* which were identified in the iron-limiting microarray play a role during uropathogenesis and will be the focus of future studies. In support of this, results of the cross-feeding assays depict *E. coli* CFT073, an enterobactin producing, yersiniabactin-negative strain, able to cross-feed *P. mirabilis* (Fig. 5D, Table 3). This suggests that *P. mirabilis*, while incapable of producing enterobactin, there is a putative TonB-dependent receptor capable of importing enterobactin. Both the *P. mirabilis* NIS type B proteobactin synthesis/receptor mutant (Pbt^{SR}) and the yersiniabactin-related synthesis/receptor mutant (Nrp^{SR}) could utilize enterobactin (Fig. 5A, Table 3). These results show that *P. mirabilis* does possess a TonB-dependent receptor or other mechanism capable of importing enterobactin. Microarray findings support this conclusion, as at least two other putative TonB-dependent receptors, PMI0842 and IreA, were up-regulated during the iron limitation. The TonB-dependent receptor Iha has been shown to function as a catecholate siderophore receptor that mediates uptake of enterobactin (Leveille *et al.*, 2006). Both PMI0842 and IreA of *P. mirabilis* have 33% and 34% identity to Iha of *E. coli*, respectively. It is likely that enterobactin is being taken up by these putative TonB-dependent receptors in *P. mirabilis*.

To investigate the role of these siderophore systems *in vivo*, independent and cochallenge competition experiments were performed with the mutant strains and wild-type HI4320. Independent challenge experiments showed that loss of both siderophore synthesis genes did not attenuate virulence. During independent challenge the yersiniabactin-related synthetase/receptor mutant (Nrp^{SR}) was recovered at modestly higher levels than wild-type HI4320 in the bladder ($P = 0.045$) and kidneys ($P = 0.036$) (Table 4). This small difference in the median CFU/g may not be biologically relevant as the ability of both Nrp^{SR} and wild-type to colonize the urinary tract was nearly indistinguishable (Fig. S2). Despite the lack of

attenuation during independent infections we found that cochallenge competition experiments between mutant and wild-type strains revealed key differences in fitness. In these experiments the proteobactin sythetase/receptor mutant (Pbt^{SR}) was able to slightly out-perform wild-type HI4320 ($P = 0.034$) where a small difference in CFUs was observed. However, these findings may also suggest the yersiniabactin-related system is predominant *in vivo* as this strain only produces the yersiniabactin-related siderophore. Consistent with this, only mutants lacking the yersiniabactin-related siderophore reduce *P. mirabilis* fitness *in vivo* (Table 5). This also agrees with a previous study from our lab, where a STM screen identified another yersiniabactin-related gene, *nrpG*, as being outcompeted by wild-type HI4320 (Himpsl *et al.*, 2008).

This study is the first genome-wide view of the *P. mirabilis* HI4320 response to iron limitation. These iron-limiting microarray findings identified systems important in ferri-siderophore uptake, heme uptake, aerobic ferrous iron uptake (Fisher et al., 2009) and ferric citrate transport (Fig. 9). This study is also the first report to demonstrate siderophore production both *in vitro* and *in vivo* by two distinct iron acquisition systems in *P. mirabilis* HI4320. Together, proteobactin and the yersiniabactin-related siderophore system, along with the numerous potential iron acquisition and transport systems identified by our microarray analysis shows that *P. mirabilis* employs a general strategy of encoding multiple systems with similar function like other extraintestinal pathogens, including uropathogenic *E. coli*.

Experimental procedures

Bacterial strains and culture conditions

Proteus mirabilis HI4230 and ten additional *P. mirabilis* caUTI isolates were isolated from urine samples from patients presenting with bacteriuria during long-term catheterization (Mobley & Warren, 1987, Warren *et al.*, 1982). *P. mirabilis* colonizing strains isolated from the anterior nares, oropharynx, groin, or wound sources (non-UTI isolates) have been previously described (Mody *et al.*, 2007). *Escherichia coli* CFT073 was isolated from the blood and urine of a patient with acute pyelonephritis (Mobley *et al.*, 1990). The *E. coli* CFT073 enterobactin and aerobactin mutant, *entF::kan iucB::cam*, has been previously described (Torres *et al.*, 2001). *E.coli* 536 has been previously described (Berger *et al.*, 1982). *E. coli* 536 *entF::kan* and *entF ybtS::kan* deletion mutants (Hagan & Mobley, unpublished) were constructed using the lambda Red recombinase system (Datsenko & Wanner, 2000). Bacteria were routinely cultured in Luria-Bertani (LB) medium (per liter, 0.5 g NaCl, 5.0 g yeast extract, 10.0 g tryptone) or on LB agar (15.0 g/L agar). Iron-limiting medium was prepared by adding 15 μM deferoxamine mesylate (Desferal) (Sigma) to LB medium. Desferal was chosen for this study based upon previous findings in which *P. mirabilis* urinary tract isolates were found to be highly susceptible to this agent (Lowy *et al.*, 1984). We determined a concentration of 15 uM Desferal in LB medium that decreased the growth rate of wild-type in comparison to wild-type grown in LB medium alone (Fig. 1). Growth curves were performed using a Bioscreen growth curve analyzer (Growth Curves) following culture of bacterial samples in triplicate. Error bars were calculated by the standard error of the mean. Iron-limited LB agar supplemented with 25 μM Desferal (Sigma) restricted *P. mirabilis* growth for siderophore cross-feeding assays. Neidhardt MOPS Minimal Medium (Neidhardt *et al.*, 1974) with and without 0.1 mM $FeCl_3{\cdot}6H_2O$ was used for culture of bacterial strains. For growth of *P. mirabilis*, Neidhardt MOPS Minimal Medium was supplemented with 1 ml 1% nicotinic acid, 1 ml 1 M MgSO4·7H20, 10 ml 20% glycerol, and 1 ml 20% chelex-treated casamino acids per liter. Chrome azurol S (CAS) agar and CAS shuttle solution was prepared as previously described (Schwyn & Neilands, 1987). Antibiotics were added as necessary at the following concentrations:

kanamycin (25 μg/ml), tetracycline (15 μg/ml), ampicillin (50 μg/ml), and chloramphenicol (20 μg/ml).

Microarray analysis

70-mer oligonucleotides representing open reading frames within the genome of *P. mirabilis* HI4320 were spotted (Microarrays, Inc.) in triplicate onto Ultra GAPSll slides (Corning) (Pearson *et al.*, 2010, Flannery *et al.*, 2009). Overnight LB medium cultures of HI4320 were diluted 1:100 in fresh LB medium or LB medium containing 15 μM of Desferal and incubated for three hours at 37°C, or until the culture reached an OD_{600} of 1.0. Cultures were treated with 2 volumes of RNA protect (Qiagen), incubated at room temperature for five minutes to stabilize RNA, and centrifuged for (10 min, 5000 × *g*, 25°C). RNA (4 μg) was purified (Qiagen) and DNase-treated (Ambion) as described above. First strand cDNA synthesis reactions, labeling of cDNA with CyDyes, and hybridization to the microarray slides were performed following the protocols; ftp://ftp.jcvi.org/pub/data/PFGRC/pdf_files/protocols/M007.pdf and ftp://ftp.jcvi.org/pub/data/PFGRC/pdf_files/protocols/M008.pdf, found on The Institute for Genomic Research (TIGR) website. The microarray was scanned by a ScanArray Express Microarray Scanner (Perkin Elmer) at 10 μm resolution.

Five independent RNA samples were subjected to microarray analysis. The cyanine 3 or cyanine 5 dye was swapped for each condition for two runs. Spot intensities were extracted and LOWESS normalized with ScanArray Express v 4.0 (Perkin Elmer) software, spot replicates were merged with Microarray Data Analysis System (MIDAS) software, and statistically analyzed using Multiexperiment Viewer (MeV) software (Saeed *et al.*, 2003). Using MeV software, a one-class unpaired test was performed by Significance Analysis of Microarray (SAM) to identify genes significantly up-regulated or down-regulated in response to *in vitro* iron limitation (Tusher *et al.*, 2001, Saeed *et al.*, 2003). The False Discovery Rate was manually set to zero. Fold-change of gene expression is presented as the $\log_2$ transformation of the ratio of the transcript level of *P. mirabilis* growth in LB medium and LB medium with Desferal, averaged across the five experiments. Microarray data are accessible through the Gene Expression Omnibus (GEO) database at with accession number GSE18051.

RNA preparation and quantitative RT-PCR

Overnight bacterial cultures were diluted 1:100 in 5 ml of fresh medium and incubated at 37°C until an OD_{600} of 1.0 was reached. A 500 μl volume of cells was treated with 62.5 μl of 5% phenol-ethanol stop solution and incubated at room temperature for 10 minutes. For RNA from *in vivo* urine samples, urine was collected into RNAprotect (Qiagen) following manufacturer's recommendation. Bacterial suspensions were centrifuged (5 min, 5000 × *g*, 4°C) and RNA was purified using an RNeasy (Qiagen) column following the manufacturer's protocol. Contaminating genomic DNA was removed with TURBO DNA-*free* (Ambion) following the manufacturer's protocol. Lack of genomic DNA contamination was determined by PCR analysis using primers to amplify the housekeeping gene *rpoA* prior to cDNA synthesis.

cDNA synthesis of total RNA was performed using SuperScript II first strand synthesis kit (Invitrogen) using 50 ng of random hexamers per 5 μg total RNA following the manufacturer's protocol. cDNA was purified on a QIAquick column (Qiagen) according to the manufacturer's protocol and eluted in 30 μl of the supplied elution buffer. Purified cDNA was quantified using a NanoDrop spectrophotometer. Transcripts were quantified on a MX3000P real-time PCR machine (Stratagene) using Brilliant SYBR green QPCR master mix (Stratagene) in 25 μl reactions containing up to 30 ng of total cDNA. Real-time

oligonucleotide sequences of genes were designed using the PrimerQuest program (Steve Rozen, Helen J. Skaletsky (1996, 1997, 1998)) on the Integrated DNA Technologies website and are listed in Table S3. Transcript levels were normalized to the housekeeping gene *rpoA* and $\log_2$ fold-change was determined relative to an experiment-specific calibrator using the MXPro v 4.1 software package (Stratagene). Error bars were calculated by the standard error of the mean and statistical analysis was performed using an unpaired *t*-test.

Reverse transcriptase PCR

Transcriptional organization of siderophore biosynthesis and ABC transport gene clusters, PMI0229-0239 and PMI2596-2605, was examined by reverse transcriptase PCR (RT-PCR) from mRNA isolated following culture of *P. mirabilis* HI4320 in LB medium with 15 μM Desferal. RNA purification, Dnase-treatment and cDNA synthesis was performed as previously described. A total of 30 ng of cDNA or genomic DNA was used in 25 μl reactions. The intergenic regions spanning genes within these systems were amplified to identify contiguous genes on the same transcript.

Mutant construction

To test siderophore production and colonization in the murine model of ascending UTI, single mutations and a double mutation of PMI0232 and PMI2599, a putative siderophore biosynthesis protein and a putative non-ribosomal peptide synthase, respectively, were constructed using the TargeTronGene Knockout System (Sigma) following a modified protocol (Pearson & Mobley, 2007). Oligonucleotides for mutant design were created using the TargeTron Design Site (Sigma) and are listed in Table S1. PCR confirmation of mutants was performed using oligonuceotides designed with the PrimerQuest program as previously described and are listed in Table S1. Mutants constructed are identified as *pbtA::kan, nrpR::kan, nrpR pbtA::kan,* and *nrpR 2596::kan*; the last two designations for these mutants refer to the *nrpR* insertion mutant with the kanamycin marker deleted and the *pbtA* or PMI2596 insertion mutant with the kanamycin marker retained. The kanamycin resistance cassette was removed from the intron by IPTG induction of the cre recombinase in pQL123 (Liu *et al.*, 1998).

Detection of siderophore production

Bacteria, cultured in LB medium with aeration at 37°C to stationary phase, were spotted in 5 μl volumes onto chrome azurol S (CAS) agar plates (Schwyn & Neilands, 1987) and incubated at 30°C for 18 hours. A visible color change of agar from blue to orange around bacterial growth indicates siderophore production. *E. coli* CFT073 and *E. coli* CFT073 *entF::kan iucB::cam*, an enterobactin aerobactin double siderophore biosynthesis mutant, were used as positive and negative controls, respectively.

For the CAS assay, overnight bacterial cultures in LB medium were diluted 1:100 into MOPS defined medium with 0.1 mM $FeCl_3{\cdot}6H_2O$. Cells were grown to stationary phase, harvested by centrifugation (5 min, 8000 × *g*, 4°C), and washed before diluting 1:100 into fresh MOPS buffer with and without 0.1mM $FeCl_3{\cdot}6H_2O$. Following growth to OD_{600} = 1.0, cells were centrifuged (20 min, 10,000 × *g*, 4°C), supernatant was collected and passed through a 0.22 μm filter (Millipore). Wild-type and mutant samples of *P. mirabilis* were lyophilized in 50 ml volumes and subsequently resuspended in 1 ml of phosphate buffered saline. A total of 150 μl of siderophore-containing supernatant was mixed with 150 μl of CAS shuttle solution as previously described (Schwyn & Neilands, 1987). Phosphate buffered saline was used for resuspension of lyophilized supernatant and phosphate buffered saline containing 15 μM Desferal served as a reference for *P. mirabilis* samples and a positive control, respectively. Following one hour incubation at room temperature, samples were measured at an absorbance of 630 nm using a MicroQuant Spectrophotometer (Bio-

Tek). Each sample was measured in triplicate. Absorbance readings were calculated by dividing the samples' averaged absorbance by the absorbance of the reference. Error bars were calculated by the standard error of the mean and statistical analysis was performed using an unpaired *t*-test.

Presence of *pbt* and *nrp* genes in other *Enterobacteriaceae*

P. mirabilis isolates were screened by PCR for the presence or absence of genes, PMI0232 and PMI2599, a putative siderophore biosynthesis protein and a putative non-ribosomal peptide synthase, respectively, using genomic DNA (Flannery *et al.*, 2009). Forward and reverse qPCR primers, *pbtA* and 2599 (Table S3), were used to amplify within the open reading frame of both genes using 60 ng of gDNA as template. Primers for amplification of PMI3255 were used as a positive DNA control as previously described (Flannery *et al.*, 2009). Associations were determined by using the Fisher exact test (GraphPad Prism).

For sequence analysis of the proteobactin synthesis protein PbtA, protein sequences homologous to PbtA were identified by BLAST (Altschul *et al.*, 1990). The resulting 92 sequences were input into MegAlign (DNASTAR) and subjected to multiple alignment using ClustalW (Thompson *et al.*, 1994) using a BLOSUM protein weight matrix and a gap penalty of 10.00. The results of the multiple alignment were used to generate a phylogenetic cladogram where the branch distances correspond to sequence divergence. The cladogram was visualized by bootstrap analysis comparing tree constructs using the neighbor-joining methodology performed with 10,000 trials initialized with a random seed.

Cross-feeding assays

Cross-feeding assays were performed to determine whether yersiniabactin produced by other bacterial species could cross-feed *P. mirabilis* HI4320. LB agar was supplemented with 25 μM Desferal, an iron-limited condition in which *P. mirabilis* was unable to grow. For cross-feeding assays, wild-type *P. mirabilis*, the proteobactin synthesis/receptor and mutant (Pbt^{SR}), and the yersiniabactin-related synthesis/receptor mutant (Nrp^{SR}) were inoculated from overnight LB medium cultures onto the surface of the iron-limited plate using a sterile 1 μl loop. *E. coli* CFT073, *E. coli* 536, and *E. coli* 536 mutant strains *entF::kan* and *entF ybtS::kan* were cross-struck from LB medium perpendicular to *P. mirabilis* strains. X-gal (40 μg/ml) was added to the iron-limited plates to distinguish growth of the *lacZ* positive, *E. coli* 536 and CFT073, and *lacZ* negative, *P. mirabilis*, strains. Following incubation at 37°C for 18 hours plates were scored for promotion of growth of the *P. mirabilis* strains.

Chromatographic detection of yersiniabactin

A final concentration of 100 μM $FeCl_3 \cdot 6H_2O$ was added to supernatants of previously described MOPS iron-depleted cultures of *E. coli* 536 mutants *entF::kan* and *entF ybtS::kan* and *P. mirabilis* mutants *pbtA::kan* and *nrpR pbtA::kan*. 50 ml of each sample were then evaporated to dryness and redissolved in 2 ml of methanol. 500 μl of this concentrated preparation was injected onto a Beckman-Coulter System Gold HPLC in line with a Waters XBridge C_{18} (4 10 × 250 mm) column running the following method: 5% acetonitrile (MeCN) in ddH_2O for 1 minute followed by a linear increase to 90% MeCN over 20 minutes and a final 3 minute 100% MeCN wash step. Peaks not shared between all samples were collected for further investigation. Prior to LC-MS analysis, concentrated supernatant samples were diluted with an equal volume of additional methanol and all insoluble material was centrifuged out of solution. 2 μl of the remaining supernatant was injected onto a Shimadzu electospray ionization (ESI) LCMS-2010A mass spectrometer in line with an HPLC system using a Phenomenex Luna C_{18} (1.5 × 250 mm) column and the following elution method: 5% (MeCN) in ddH_2O for 10 minutes (over which time material was diverted from the detector) followed by a jump to 20% MeCN and increasing by a linear

gradient to 95% MeCN over 30 minutes. Detection occurred in positive scanning and selected ion monitoring (SIM) modes. Collected peaks from previous HPLC analysis were evaporated under N_2, redissolved in methanol, and analyzed by LC-MS in an identical manner.

CBA/J mouse model of ascending UTI

The CBA mouse model of ascending UTI (Johnson *et al.*, 1987, Hagberg *et al.*, 1983) was used to assess the contribution to fitness and virulence of the siderophore biosynthesis and ABC transport systems. For cochallenge competition (to determine fitness) experiments, 6–8 week old female CBA/J mice (20 to 22 g; Jackson Laboratories) were transurethrally infected with a 50 μl bacterial suspension of 5×10^7 CFU containing a 1:1 ratio of *P. mirabilis* HI4320 and *P. mirabilis* antibiotic-resistant mutant. For independent challenge (to determine virulence) mice were infected with wild-type HI4320 alone or mutant alone. Urine was collected and pooled from mice infected with wild-type *P. mirabilis* HI4320 at 24 hours, 48 hours, and 5 days post-infection for transcriptional analysis. Mice were euthanized 7 days post infection. Bladder and kidneys were collected, homogenized, and plated on plain LB agar and/or LB agar with antibiotic (Autoplate 4000, SpiralBiotech). Viable colony counts were enumerated using a Q Count (Spiral Biotech) and expressed as CFU/g of tissue. For cochallenge competition experiments, wild-type infection was determined by subtracting the number of colonies on LB agar containing antibiotic from the number of colonies on plain LB agar. Competitive indices (CI) were calculated by dividing the ratio of the CFU of wild-type to mutant recovered from mice following infection by the ratio of the CFU of wild-type HI4320 to the CFU of mutant present in the input. A CI > 1 indicates the wild-type out-competes the mutant strain and a CI < 1 indicates the wild-type is out-competed by the mutant. The Mann-Whitney test was used to determine the statistical significance of data obtained in independent challenge experiments and cochallenge competition experiments were analyzed using the Wilcoxon signed-rank test.

Supplementary Material

Refer to Web version on PubMed Central for supplementary material.

Acknowledgments

The authors would like to thank Shelley Payne for helpful procedural advice regarding CAS agar, Alfredo Torres for generously providing the CFT073 *entF::kan iucB::cam* strain, Erin Hagan for construction of *E. coli* 536 mutants *entF::kan* and *entF ybtS::kan* and helpful insight to the study, Lona Mody for generously providing *P. mirabilis* non-UTI colonizing isolates, Sara Smith for assistance with our animal studies, and Chris Alteri for critical reading of the manuscript.

This study was supported in part by the Public Health Service Grants AI043360 and AI059722 from the National Institutes of Health.

References

Alteri CJ, Mobley HL. Quantitative profile of the uropathogenic *Escherichia coli* outer membrane proteome during growth in human urine. Infection and immunity. 2007; 75:2679–2688. [PubMed: 17513849]

Altschul SF, Gish W, Miller W, Myers EW, Lipman DJ. Basic local alignment search tool. Journal of molecular biology. 1990; 215:403–410. [PubMed: 2231712]

Andrews SC, Robinson AK, Rodriguez-Quinones F. Bacterial iron homeostasis. FEMS microbiology reviews. 2003; 27:215–237. [PubMed: 12829269]

Berger H, Hacker J, Juarez A, Hughes C, Goebel W. Cloning of the chromosomal determinants encoding hemolysin production and mannose-resistant hemagglutination in *Escherichia coli*. Journal of bacteriology. 1982; 152:1241–1247. [PubMed: 6754701]

Braun V. Energy-coupled transport and signal transduction through the gram-negative outer membrane via TonB-ExbB-ExbD-dependent receptor proteins. FEMS microbiology reviews. 1995; 16:295–307. [PubMed: 7654405]

Brzuszkiewicz E, Bruggemann H, Liesegang H, Emmerth M, Olschlager T, Nagy G, Albermann K, Wagner C, Buchrieser C, Emody L, Gottschalk G, Hacker J, Dobrindt U. How to become a uropathogen: comparative genomic analysis of extraintestinal pathogenic *Escherichia coli* strains. Proceedings of the National Academy of Sciences of the United States of America. 2006; 103:12879–12884. [PubMed: 16912116]

Bultreys A, Gheysen I, de Hoffmann E. Yersiniabactin production by *Pseudomonas syringae* and *Escherichia coli*, and description of a second yersiniabactin locus evolutionary group. Appl Environ Microbiol. 2006; 72:3814–3825. [PubMed: 16751485]

Burall LS, Harro JM, Li X, Lockatell CV, Himpsl SD, Hebel JR, Johnson DE, Mobley HL. *Proteus mirabilis* genes that contribute to pathogenesis of urinary tract infection: identification of 25 signature-tagged mutants attenuated at least 100-fold. Infection and immunity. 2004; 72:2922–2938. [PubMed: 15102805]

Carniel E, Guilvout I, Prentice M. Characterization of a large chromosomal “high-pathogenicity island” in biotype 1B *Yersinia enterocolitica*. Journal of bacteriology. 1996; 178:6743–6751. [PubMed: 8955291]

Challis GL. A widely distributed bacterial pathway for siderophore biosynthesis independent of nonribosomal peptide synthetases. Chembiochem. 2005; 6:601–611. [PubMed: 15719346]

Crosa JH, Walsh CT. Genetics and assembly line enzymology of siderophore biosynthesis in bacteria. Microbiol Mol Biol Rev. 2002; 66:223–249. [PubMed: 12040125]

Datsenko KA, Wanner BL. One-step inactivation of chromosomal genes in *Escherichia coli* K-12 using PCR products. Proceedings of the National Academy of Sciences of the United States of America. 2000; 97:6640–6645. [PubMed: 10829079]

Drechsel H, Thieken A, Reissbrodt R, Jung G, Winkelmann G. Alpha-keto acids are novel siderophores in the genera *Proteus*, *Providencia*, and *Morganella* and are produced by amino acid deaminases. Journal of bacteriology. 1993; 175:2727–2733. [PubMed: 8478334]

Ernst JF, Bennett RL, Rothfield LI. Constitutive expression of the iron-enterochelin and ferrichrome uptake systems in a mutant strain of *Salmonella typhimurium*. Journal of bacteriology. 1978; 135:928–934. [PubMed: 151097]

Evanylo LP, Kadis S, Maudsley JR. Siderophore production by *Proteus mirabilis*. Canadian journal of microbiology. 1984; 30:1046–1051. [PubMed: 6238666]

Faraldo-Gomez JD, Sansom MS. Acquisition of siderophores in gram-negative bacteria. Nat Rev Mol Cell Biol. 2003; 4:105–116. [PubMed: 12563288]

Fisher CR, Davies NM, Wyckoff EE, Feng Z, Oaks EV, Payne SM. Genetics and virulence association of the *Shigella flexneri sit* iron transport system. Infection and immunity. 2009; 77:1992–1999. [PubMed: 19289511]

Flannery EL, Mody L, Mobley HL. Identification of a modular pathogenicity island that is widespread among urease-producing uropathogens and shares features with a diverse group of mobile elements. Infection and immunity. 2009; 77:4887–4894. [PubMed: 19687197]

Franza T, Mahe B, Expert D. *Erwinia chrysanthemi* requires a second iron transport route dependent of the siderophore achromobactin for extracellular growth and plant infection. Molecular microbiology. 2005; 55:261–275. [PubMed: 15612933]

Gaisser S, Hughes C. A locus coding for putative non-ribosomal peptide/polyketide synthase functions is mutated in a swarming-defective *Proteus mirabilis* strain. Mol Gen Genet. 1997; 253:415–427. [PubMed: 9037101]

Hagan EC, Mobley HL. Haem acquisition is facilitated by a novel receptor Hma and required by uropathogenic *Escherichia coli* for kidney infection. Molecular microbiology. 2009; 71:79–91. [PubMed: 19019144]

Hagberg L, Engberg I, Freter R, Lam J, Olling S, Svanborg Eden C. Ascending, unobstructed urinary tract infection in mice caused by pyelonephritogenic *Escherichia coli* of human origin. Infection and immunity. 1983; 40:273–283. [PubMed: 6339403]

Hantke K. Iron and metal regulation in bacteria. Current opinion in microbiology. 2001; 4:172–177. [PubMed: 11282473]

Himpsl SD, Lockatell CV, Hebel JR, Johnson DE, Mobley HL. Identification of virulence determinants in uropathogenic *Proteus mirabilis* using signature-tagged mutagenesis. Journal of medical microbiology. 2008; 57:1068–1078. [PubMed: 18719175]

Johnson DE, Lockatell CV, Hall-Craigs M, Mobley HL, Warren JW. Uropathogenicity in rats and mice of *Providencia stuartii* from long-term catheterized patients. The Journal of urology. 1987; 138:632–635. [PubMed: 3625871]

Jones AM, Lindow SE, Wildermuth MC. Salicylic acid, yersiniabactin, and pyoverdin production by the model phytopathogen *Pseudomonas syringae* pv. tomato DC3000: synthesis, regulation, and impact on tomato and *Arabidopsis* host plants. Journal of bacteriology. 2007; 189:6773–6786. [PubMed: 17660289]

Kessler D. Enzymatic activation of sulfur for incorporation into biomolecules in prokaryotes. FEMS microbiology reviews. 2006; 30:825–840. [PubMed: 17064282]

Koster W. ABC transporter-mediated uptake of iron, siderophores, heme and vitamin B12. Research in microbiology. 2001; 152:291–301. [PubMed: 11421276]

Leveille S, Caza M, Johnson JR, Clabots C, Sabri M, Dozois CM. Iha from an *Escherichia coli* urinary tract infection outbreak clonal group A strain is expressed *in vivo* in the mouse urinary tract and functions as a catecholate siderophore receptor. Infection and immunity. 2006; 74:3427–3436. [PubMed: 16714573]

Lima A, Zunino P, D'Alessandro B, Piccini C. An iron-regulated outer-membrane protein of *Proteus mirabilis* is a haem receptor that plays an important role in urinary tract infection and in in vivo growth. Journal of medical microbiology. 2007; 56:1600–1607. [PubMed: 18033826]

Liu Q, Li MZ, Leibham D, Cortez D, Elledge SJ. The univector plasmid-fusion system, a method for rapid construction of recombinant DNA without restriction enzymes. Curr Biol. 1998; 8:1300–1309. [PubMed: 9843682]

Lowy FD, Pollack S, Fadl-Allah N, Steigbigel NH. Susceptibilities of bacterial and fungal urinary tract isolates to desferrioxamine. Antimicrobial agents and chemotherapy. 1984; 25:375–376. [PubMed: 6721470]

Marcelis JH, den Daas-Slagt HJ, Hoogkamp-Korstanje JA. Iron requirement and chelator production of *staphylococci*, *Streptococcus faecalis* and *enterobacteriaceae*. Antonie van Leeuwenhoek. 1978; 44:257–267. [PubMed: 110252]

Massad G, Zhao H, Mobley HL. *Proteus mirabilis* amino acid deaminase: cloning, nucleotide sequence, and characterization of *aad*. Journal of bacteriology. 1995; 177:5878–5883. [PubMed: 7592338]

Miethke M, Marahiel MA. Siderophore-based iron acquisition and pathogen control. Microbiol Mol Biol Rev. 2007; 71:413–451. [PubMed: 17804665]

Mihara H, Muramatsu H, Kakutani R, Yasuda M, Ueda M, Kurihara T, Esaki N. N-methyl-L-amino acid dehydrogenase from *Pseudomonas putida*. A novel member of an unusual NAD(P)-dependent oxidoreductase superfamily. The FEBS journal. 2005; 272:1117–1123. [PubMed: 15720386]

Miles AA, Khimji PL. Enterobacterial chelators of iron: their occurrence, detection, and relation to pathogenicity. Journal of medical microbiology. 1975; 8:477–490. [PubMed: 812996]

Mobley HL, Green DM, Trifillis AL, Johnson DE, Chippendale GR, Lockatell CV, Jones BD, Warren JW. Pyelonephritogenic *Escherichia coli* and killing of cultured human renal proximal tubular epithelial cells: role of hemolysin in some strains. Infection and immunity. 1990; 58:1281–1289. [PubMed: 2182540]

Mobley HL, Warren JW. Urease-positive bacteriuria and obstruction of long-term urinary catheters. Journal of clinical microbiology. 1987; 25:2216–2217. [PubMed: 3320089]

Mody L, Maheshwari S, Galecki A, Kauffman CA, Bradley SF. Indwelling device use and antibiotic resistance in nursing homes: identifying a high-risk group. Journal of the American Geriatrics Society. 2007; 55:1921–1926. [PubMed: 18081670]

Munch R, Hiller K, Grote A, Scheer M, Klein J, Schobert M, Jahn D. Virtual Footprint and PRODORIC: an integrative framework for regulon prediction in prokaryotes. Bioinformatics (Oxford, England). 2005; 21:4187–4189.

Munzinger M, Budzikiewicz H, Expert D, Enard C, Meyer JM. Achromobactin, a new citrate siderophore of *Erwinia chrysanthemi*. Zeitschrift fur Naturforschung. 2000; 55:328–332. [PubMed: 10928541]

Neidhardt FC, Bloch PL, Smith DF. Culture medium for *enterobacteria*. Journal of bacteriology. 1974; 119:736–747. [PubMed: 4604283]

Neilands JB. Siderophores: structure and function of microbial iron transport compounds. The Journal of biological chemistry. 1995; 270:26723–26726. [PubMed: 7592901]

Oves-Costales D, Kadi N, Challis GL. The long-overlooked enzymology of a nonribosomal peptide synthetase-independent pathway for virulence-conferring siderophore biosynthesis. Chemical communications (Cambridge, England). 2009:6530–6541.

Pearson MM, Mobley HL. The type III secretion system of *Proteus mirabilis* HI4320 does not contribute to virulence in the mouse model of ascending urinary tract infection. Journal of medical microbiology. 2007; 56:1277–1283. [PubMed: 17893161]

Pearson MM, Rasko DA, Smith SN, Mobley HL. Transcriptome of swarming *Proteus mirabilis*. Infection and immunity. 2010; 78:2834–2845. [PubMed: 20368347]

Pearson MM, Sebaihia M, Churcher C, Quail MA, Seshasayee AS, Luscombe NM, Abdellah Z, Arrosmith C, Atkin B, Chillingworth T, Hauser H, Jagels K, Moule S, Mungall K, Norbertczak H, Rabbinowitsch E, Walker D, Whithead S, Thomson NR, Rather PN, Parkhill J, Mobley HL. Complete genome sequence of uropathogenic *Proteus mirabilis*, a master of both adherence and motility. Journal of bacteriology. 2008; 190:4027–4037. [PubMed: 18375554]

Piccini CD, Barbe FM, Legnani-Fajardo CL. Identification of iron-regulated outer membrane proteins in uropathogenic *Proteus mirabilis* and its relationship with heme uptake. FEMS microbiology letters. 1998; 166:243–248. [PubMed: 9770281]

Ratledge C, Dover LG. Iron metabolism in pathogenic bacteria. Annual review of microbiology. 2000; 54:881–941.

Saeed AI, Sharov V, White J, Li J, Liang W, Bhagabati N, Braisted J, Klapa M, Currier T, Thiagarajan M, Sturn A, Snuffin M, Rezantsev A, Popov D, Ryltsov A, Kostukovich E, Borisovsky I, Liu Z, Vinsavich A, Trush V, Quackenbush J. TM4: a free, open-source system for microarray data management and analysis. BioTechniques. 2003; 34:374–378. [PubMed: 12613259]

Schmelz S, Kadi N, McMahon SA, Song L, Oves-Costales D, Oke M, Liu H, Johnson KA, Carter LG, Botting CH, White MF, Challis GL, Naismith JH. AcsD catalyzes enantioselective citrate desymmetrization in siderophore biosynthesis. Nature chemical biology. 2009; 5:174–182.

Schwyn B, Neilands JB. Universal chemical assay for the detection and determination of siderophores. Analytical biochemistry. 1987; 160:47–56. [PubMed: 2952030]

Shand GH, Anwar H, Kadurugamuwa J, Brown MR, Silverman SH, Melling J. *In vivo* evidence that bacteria in urinary tract infection grow under iron-restricted conditions. Infection and immunity. 1985; 48:35–39. [PubMed: 3980092]

Snyder JA, Haugen BJ, Buckles EL, Lockatell CV, Johnson DE, Donnenberg MS, Welch RA, Mobley HL. Transcriptome of uropathogenic *Escherichia coli* during urinary tract infection. Infection and immunity. 2004; 72:6373–6381. [PubMed: 15501767]

Thompson JD, Higgins DG, Gibson TJ. CLUSTAL W: improving the sensitivity of progressive multiple sequence alignment through sequence weighting, position-specific gap penalties and weight matrix choice. Nucleic Acids Res. 1994; 22:4673–4680. [PubMed: 7984417]

Torres AG, Redford P, Welch RA, Payne SM. TonB-dependent systems of uropathogenic *Escherichia coli:* aerobactin and heme transport and TonB are required for virulence in the mouse. Infection and immunity. 2001; 69:6179–6185. [PubMed: 11553558]

Tuckman M, Osburne MS. *In vivo* inhibition of TonB-dependent processes by a TonB box consensus pentapeptide. Journal of bacteriology. 1992; 174:320–323. [PubMed: 1729219]

Tusher VG, Tibshirani R, Chu G. Significance analysis of microarrays applied to the ionizing radiation response. Proceedings of the National Academy of Sciences of the United States of America. 2001; 98:5116–5121. [PubMed: 11309499]

Wandersman C, Delepelaire P. Bacterial iron sources: from siderophores to hemophores. Annual review of microbiology. 2004; 58:611–647.

Warren JW, Tenney JH, Hoopes JM, Muncie HL, Anthony WC. A prospective microbiologic study of bacteriuria in patients with chronic indwelling urethral catheters. The Journal of infectious diseases. 1982; 146:719–723. [PubMed: 6815281]

Winkelmann G. Microbial siderophore-mediated transport. Biochemical Society transactions. 2002; 30:691–696. [PubMed: 12196166]

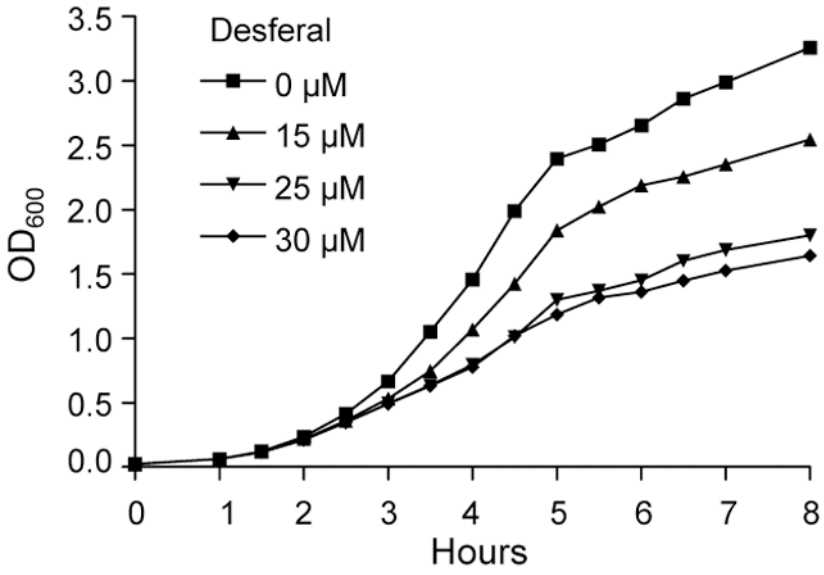

Fig. 1. The growth rate of *P. mirabilis* HI4320 is decreased following culture in LB medium containing Desferal

P. mirabilis HI4320 cultured in LB medium containing 0, 15, 25, or 30 μM Desferal, an iron-chelating agent. A concentration of 15 uM Desferal in LB medium decreases the growth rate of wild-type in comparison to wild-type grown in LB medium alone.

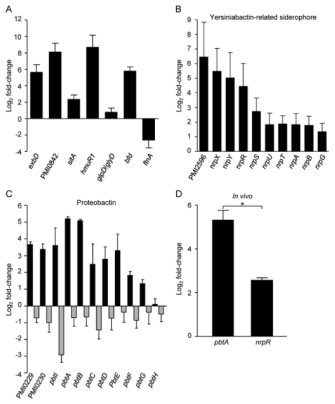

Fig. 2. qPCR of mRNA from *P. mirabilis* HI4320 cultured in LB medium containing 15 μM Desferal validates microarray results that identified up- and down-regulated genes in response to iron limitation

Log_2 fold-change was determined relative to strain HI4320 cultured in LB medium alone. (A) qPCR validation of select HI4320 genes up- or down-regulated during iron limitation *in vitro* as determined by microarray. (B) qPCR validation of HI4320 putative yersiniabactin-related siderophore, *nrp* (PMI2596-2605) that was up-regulated during iron limitation *in vitro* as determined by microarray. (C) qPCR validation of HI4320 putative siderophore system proteobactin, *pbt* (PMI0229-0239) that was up-regulated during iron limitation *in vitro* as determined by microarray (black bars) and down-regulated following the addition of 25 μM $FeCl_3 \cdot 6H_2O$ to an iron-chelated LB medium culture of bacteria (grey bars). (D) qPCR confirmation of HI4320 siderophore biosynthesis genes *pbtA* (PMI0232) and *nrpR* (PMI2599) expression *in vivo*. mRNA, isolated from bacteria recovered from the urine of experimentally infected CBA/J mice, was subjected to qPCR. A significant difference in expression levels (*, $P = 0.0002$) was determined using a two-tailed unpaired *t*-test.

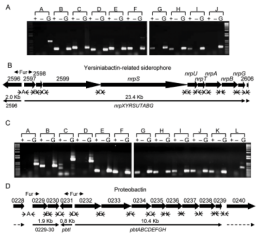

Fig. 3. Transcriptional organization of putative siderophore system PMI2596-2605 and PMI0229-0239 in *P. mirabilis* HI4320

(A, C) mRNA for cDNA synthesis was isolated from wild-type HI4320 following culture in LB medium containing15 μM Desferal. For PCR reactions: +, reverse transcriptase added to cDNA synthesis reaction; −, no reverse transcriptase added, mRNA used as template; G, HI4320 genomic DNA used as template. (B, D) Siderophore biosynthesis and transport gene clusters of HI4320 drawn to scale with primer design for RT-PCR operon mapping. Thick arrows represent open reading frames that indicate direction of transcription. Ferric uptake regulator (Fur) recognition sequences were identified based on homology to those of *P. aeruginosa* using a promoter analysis program in the Virtual Footprint software suite (Munch *et al.*, 2005). Location and direction of Fur recognition sequences are indicated. Intergenic primer pairs used for RT-PCR are represented by alphabetical letters. Thin solid arrows represent direction and span the length of genes that are required to make a complete transcript. Proposed gene nomenclature for transcripts are indicated below thin solid lines and size of transcript are indicated above the solid lines.

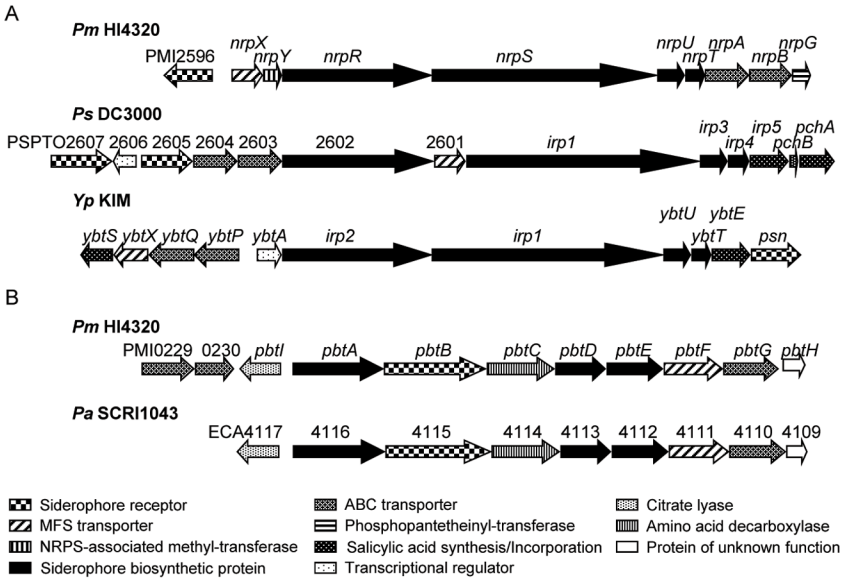

Fig. 4. The yersiniabactin-related siderophore and proteobactin of *P. mirabilis* are similar to siderophore biosynthesis and transport gene clusters in other *Enterobacteriaceae* as shown by gene sequence alignments

(A) *P. mirabilis* yersiniabactin-related siderophore is homologous to that of *P. syringae* DC3000 and *Y. pestis* KIM. The yersiniabactin-related siderophore of *P. mirabilis* lacks the genes involved in salicyclic acid biosynthesis and incorporation, *ybtS* and *ybtE* of *Y. pestis* and *irp5*, *pchB*, and *pchA* of *P. syringae*. The *nrp* locus of *P. mirabilis* also lacks a transcriptional regulator but encodes a NRPS-associated methyl-transferase and a phosphopantetheinyl-transferase which are not located within the yersiniabactin operons of *P. syringae* and *Y. pestis*. (B) The newly identified NIS system of *P. mirabilis*, proteobactin, is similar to identical gene clusters found in *P. carotovora* subsp. *atroseptica* (shown) and *P. carotovora* subsp. *carotovora*.

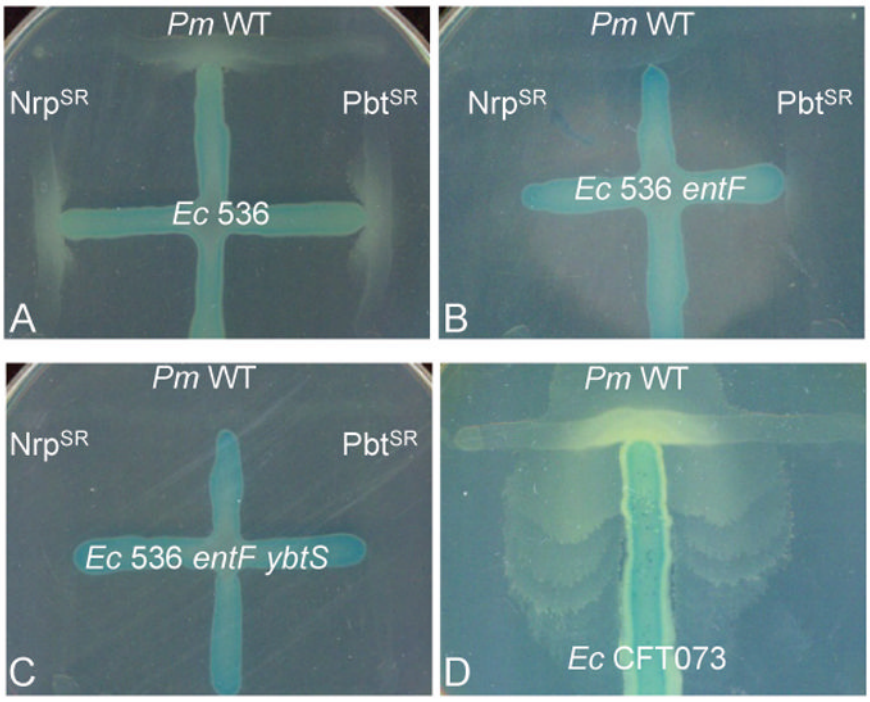

Fig. 5. *P. mirabilis* is unable to utilize yersiniabactin produced by uropathogenic *E. coli* 536

LB medium was supplemented with 25 μM Desferal, the minimum concentration of chelator required to completely suppress growth of *P. mirabilis*. Lactose-fermenting *E. coli* are distinguished from *P. mirabilis* by the using the chromogenic indicator X-gal. (A) Growth of wild-type *P. mirabilis*, the proteobactin synthesis/receptor mutant (Pbt^{SR}), and the yersiniabactin-related siderophore/receptor mutant (Nrp^{SR}) can be restored when cross-fed by *E. coli* 536 that produces both enterobactin and yersiniabactin. (B, C) Restoration of *P. mirabilis* growth for all strains tested is abolished when cross-fed by the either *E. coli* 536 enterobactin mutant, *entF::kan*, or the enterobactin/yersiniabactin double mutant, *entF ybtS::kan*. (D) *P. mirabilis* growth can be restored using *E. coli* CFT073, an enterobactin producing strain incapable of synthesizing yersiniabactin.

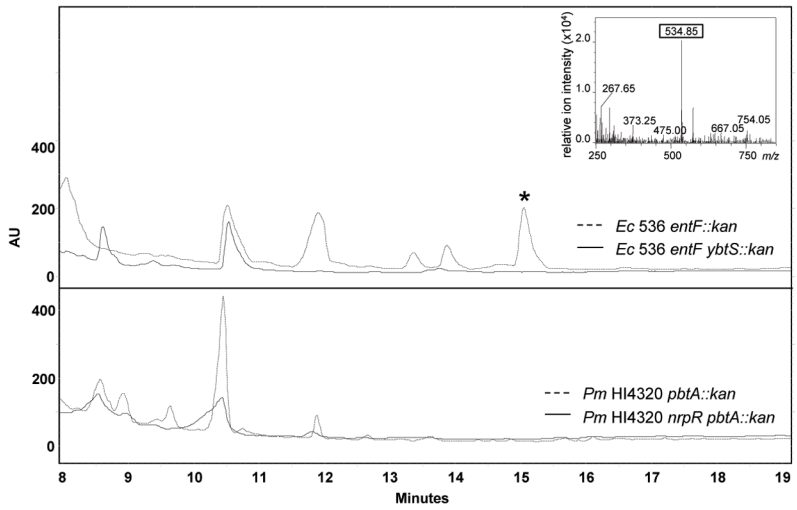

Fig. 6. Preparative HPLC and LC-MS analysis demonstrates *P. mirabilis* HI4230 is incapable of producing yersiniabactin

Preparative HPLC chromatogram (upper traces) performed on crude supernatant extracts from yersiniabactin-producing *E. coli* 536 *entF::kan* (dashed line) and yersiniabactin-deficient *entF ybtS::kan* (solid line) cultures to demonstrate production/lack of production of yersiniabactin. The lower traces represent chromatograms using the same HPLC conditions from *P. mirabilis* HI4230 *pbtA::kan* (dashed line) and *nrpR pbtA::kan* (solid line). The y-axis represents arbitrary units (AU) to offset sample traces. The inset indicates the LC-MS (positive ion mode) analysis of *E. coli* yersiniabactin present in the dominant peak (*) isolated at 15 min by HPLC. Iron-bound yersiniabactin is known to have an ion intensity at *m/z* of 535.1.

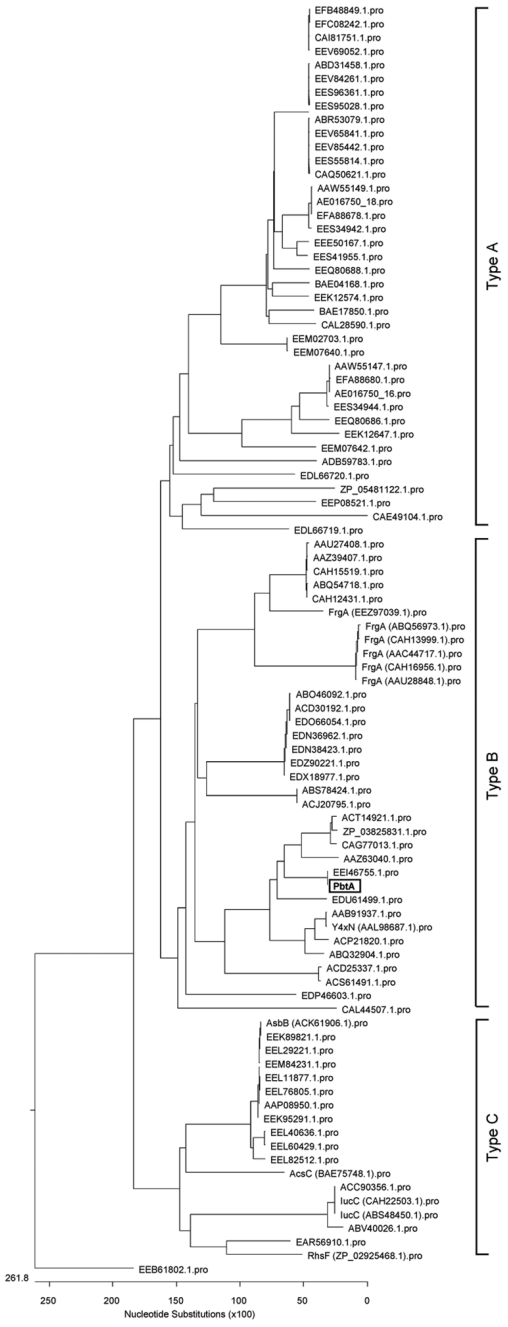

Fig. 7. Phylogenetic analysis of 92 homologous protein sequences to NIS synthetase PbtA involved in the assembly of proteobactin

The NIS synthetase enzymes are split into three subfamilies A, B, and C. Proteobactin synthetase, PbtA, (boxed) is placed with the type B subfamily clade of NIS synthetases which includes Y4xN, a siderophore synthetase previously found to be homologous to other NIS synthetases of this group.

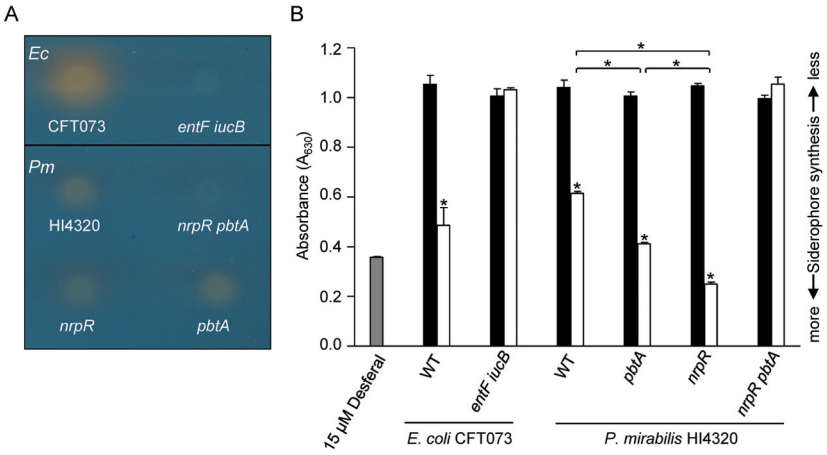

Fig. 8. Siderophore production by *P. mirabilis* HI4320

(A) Detectable siderophore production on chrome azurol S (CAS) agar of overnight LB bacterial cultures spotted in 5 μl volumes. Blue to orange color change of agar indicates siderophore production. (B) CAS assay depicting siderophore production from filtered bacterial supernatants following culture in MOPS defined medium with (black bars) and without (white bars) 0.1 mM $FeCl_3 \cdot 6H_2O$. Only supernatants of *P. mirabilis* samples were concentrated 50-fold. Supernatant of *E. coli* CFT073 and double mutant, *entF::kan iucB::cam*, were not concentrated. Positive control of phosphate buffered saline containing 15 μM Desferal (grey bar). A lower absorbance (A_{630}) indicates greater siderophore production. Significant differences in absorbance (*, $P \leq 0.0022$) was determined using a two-tailed unpaired *t*-test.

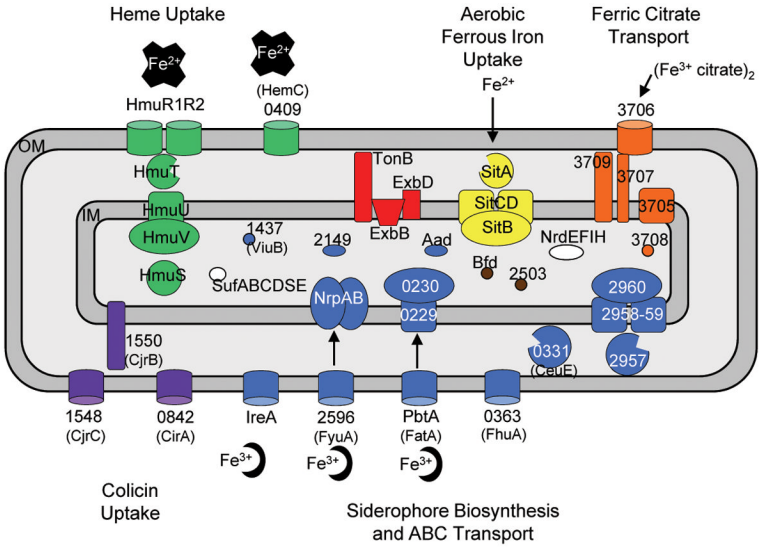

Fig. 9. A proposed model for iron acquisition systems in *P. mirabilis*

Hypothetical functions of the proteins listed are based on up-regulation of their genes under iron limitation, homology with genes from other bacterial species, and functional studies conducted in this report and related bacterial species. Outer membrane (OM) receptors are dependent on the energy transducing complex TonB-ExbB-ExbD (shown in red) for intracellular transport of iron. Heme uptake systems are displayed in green. Heme uptake may also be carried out by the outer membrane receptor, HemC. Import of periplasmic ferrous iron is performed by the ABC transporter SitABCD (shown in yellow) located on the inner membrane (IM). A putative ferric citrate system (shown in orange) encodes a TonB-dependent receptor PMI3706, and accessory proteins. Proteins involved in siderophore biosynthesis and transport of ferri-siderophores are shown in blue. Ferri-siderophores are transported by outer membrane receptors IreA, FyuA, FatA, and FhuA. Ferri-siderophores transported to the periplasm are shuttled to inner membrane transport proteins, NrpAB and PMI0229-0230. Additional putative ferri-siderophore transport proteins include the periplasmic binding protein, CeuE, and inner membrane transport proteins, PMI2957-2960. Cellular proteins, Aad, PMI2149, ViuB and, may be involved in siderophore synthesis and the regulation and utilization of iron of ferri-siderophore. Putative TonB-dependent receptors possibly involved in colicin uptake are shown in purple. Cytoplasmic iron-containing proteins include *nrdEFIH* and *sufABCDSE* (shown in white). Bfd, an iron removal protein, and PMI2503 involved in iron metabolism are shown in brown.

Table 1

Putative iron acquisition systems up-regulated in *P. mirabilis* HI4320 during iron-limiting microarray[a]

Function[b]	PMI no.	Gene	Description	Log_2 fold-change[c]
Heme uptake	0409*		putative TonB-dependent heme receptor	6.22
	1424*		putative hemin uptake protein	8.52
	1425*	*hmuR1*	hemin receptor	5.92
	1426*	*hmuR2*	hemin receptor	7.89
	1427*	*hmuS*	hemin transport protein	6.96
	1428*	*hmuT*	hemin binding periplasmic protein	5.02
	1429	*hmuU*	hemin transport system; permease protein	3.42
	1430*	*hmuV*	hemin transport system; ATP-binding protein	5.42
Ferrous iron uptake	1024	*sitD*	iron ABC transporter; membrane protein	3.41
	1025	*sitC*	iron ABC transporter; membrane protein	4.81
	1026*	*sitB*	iron ABC transporter; ATP-binding protein	5.49
	1027	*sitA*	iron ABC transporter; periplasmic substrate binding protein	5.93
Ferric citrate transport	3704		exported protease	1.36
	3705		putative ABC transport binding protein	2.14
	3706		TonB-dependent receptor	2.45
	3707		FecR-transcriptional regulator	3.83
	3708		extracytoplasmic function (EFC)-family σ factor	4.52
	3709		TonB-like protein	2.92
Putative siderophore biosynthesis & ABC transport systems	0229*		ABC transporter; permease protein	4.81
	0230		ATP-binding protein	3.94
	0231*	*pbtI*	putative citrate lyase β subunit	6.45
	0232*	*pbtA*	putative siderophore biosynthesis protein	6.36
	0233*	*pbtB*	putative TonB-dependent siderophore receptor	6.04
	0234*	*pbtC*	putative lysine/ornithine decarboxylase	5.30
	0235*	*pbtD*	putative pyridoxal-phosphate dependent enzyme	4.77
	0236	*pbtE*	putative octopine/opine/tauropine dehydrogenase	3.23
	0237	*pbtF*	MFS-family transporter	3.31
	0238	*pbtG*	putative substrate-binding protein	1.76
	0239	*pbtH*	conserved hypothetical protein	2.53
	2596*		putative siderophore TonB-dependent receptor	7.13
	2597	*nrpX*	MFS-family transporter	5.92
	2598*	*nrpY*	conserved hypothetical protein	7.93
	2599	*nrpR*	putative nonribosomal peptide synthase	5.15

Function[b]	PMI no.	Gene	Description	Log_2 fold-change[c]
	2600	*nrpS*	putative nonribosomal peptide synthase	3.62
	2601	*nrpU*	putative siderophore biosynthetic protein	2.92
	2602	*nrpT*	putative siderophore biosynthetic protein (thioesterase)	2.90
	2603	*nrpA*	put. sid. ABC transporter; ATP-binding/permease protein	4.08
	2604	*nrpB*	put. sid. ABC transporter; ATP-binding/permease protein	3.56
	2605	*nrpG*	putative 4′-phosphopantetheinyl transferase	1.27
Additional ferri-siderophore transporters	0331*		putative ABC transporter; substrate binding protein	6.49
	0363		putative TonB-dependent ferri-siderophore receptor	3.52
	1945*	*ireA*	putative TonB-dependent ferri-siderophore receptor	6.65
	2957*		putative iron ABC transporter; substrate binding protein	6.20
	2958		putative iron ABC transporter; permease component	3.93
	2959		putative iron ABC transporter; permease	2.99
	2960		putative iron ABC transporter; ATP-binding	3.13

[a] Putative iron acquisition systems of *P. mirabilis* HI4320 listed are composed of genes that were up-regulated during *in vitro* iron limitation with a fold-change ≥ 2-fold.

[b] Genes are grouped by function and listed within putative systems or operons by ascending *P. mirabilis* gene identification number (PMI no.).

[c] Log_2 transformation of fold-change values determined by taking ratio of transcript level of *P. mirabilis* growth in LB medium and LB medium treated with 15 μM Desferal averaged across all five microarray experiments.

* Genes found to be significantly up-regulated as determined by Significance Analysis of Microarray (SAM).

Table 2

Similarity search between *P. mirabilis* and *Y. pestis*, *E. coli*, *P. syringae*, and *P. luminescens*.

Gene (No. of amino acids)	% Identity (% Similarity)		No. of Amino acids
PMI2596 (662)			
	Yp KIM *psn*	27 (48)	673
	Ec 536 ECP_1947	27 (49)	673
	Ps DC3000 PSPTO2605	27 (47)	685
	Pl TT01 Plu2316	30 (46)	668
PMI2597 *nrpX* (409)			
	Yp KIM *ybtX*	39 (58)	467
	Ec 536 *ybtX*	38 (58)	462
	Ps DC3000 PSPTO2601	25 (46)	408
	Pl TT01 Plu2317	31 (53)	414
* PMI2598 *nrpY* (245)			
	Yp KIM y0042	34 (51)	260
	Ec 536 ECP_3773	34 (51)	260
	Ps DC3000 *argS*	26 (44)	578
	Pl TT01 Plu2237	40 (59)	315
PMI2599 *nrpR* (2034)			
	Yp KIM *irp2*	40 (59)	2035
	Ec 536 HMWP2	40 (59)	2035
	Ps DC3000 PSPTO2602	42 (59)	2057
	Pl TT01 Plu2320	41 (58)	2049
PMI2600 *nrpS* (3071)			
	Yp KIM *irp1*	50 (66)	3163
	Ec 536 HMWP1	50 (66)	3163
	Ps DC3000 *irp1*	52 (67)	3173
	Pl TT01 Plu2321	39 (56)	3908
PMI2601 *nrpU* (362)			
	Yp KIM *ybtU*	42 (64)	386
	Ec 536 *ybtU*	42 (64)	366
	Ps DC3000 *irp3*	44 (62)	360
	Pl TT01 Plu2322	38 (57)	365
PMI2602 *nrpT* (257)			
	Yp KIM *ybtT*	47 (58)	218
	Ec 536 *ybtT*	44 (57)	262
	Ps DC3000 *irp4*	48 (61)	271
	Pl TT01 Plu2323	47 (57)	258
PMI2603 *nrpB* (588)			
	Yp KIM *ybtP*	30 (53)	600
	Ec 536 *ybtP*	30 (53)	570
	Ps DC3000 PSPTO2604	45 (67)	593

Gene (No. of amino acids)	% Identity (% Similarity)		No. of Amino acids
	Pl TT01 Plu2318	31(52)	572
PMI2604 *nrpA* (575)			
	Yp KIM ybtQ	32 (56)	600
	Ec 536 ybtQ	32 (57)	600
	Ps DC3000 PSPTO2603	46 (68)	581
	Pl TT01 Plu2319	31 (52)	600
* PMI2605 (249)			
	Yp KIM y1938	35 (52)	410
	Ec 536 ECP_1982	38 (62)	62
	Ps DC3000 *bphP*	43 (56)	745
	Pl TT01 Plu4193	31 (46)	237

* *P. mirabilis* gene listed has homology to genes located outside of the yersiniabactin operon of other *Enterobacteriaceae.*

Table 3

Cross-feeding of *P. mirabilis* wild-type and siderophore mutants by *E.coli* 536, 536 siderophore mutants, and CFT073.

	Ability to cross-feed *P. mirabilis* strains			
	***E. coli* 536**	***E. coli* 536 *entF::kan***	***E. coli* 536 *entF ybtS::kan***	***E. coli* CFT073**
P. mirabilis	+	−	−	+
P. mirabilis Pbt^{SR}	+	−	−	+
P. mirabilis Nrp^{SR}	+	−	−	+

Strain noted as synthetase^{S} and receptor^{R} mutant in the proteobactin (Pbt) and/or yersiniabactin-related (Nrp) siderophore system.

+, growth

−, no growth

Table 4

In vivo virulence of siderophore biosynthesis mutants following independent challenge experiments.

Strain defect[a]	Bladder		Kidneys	
	Median CFU	*P*-value[b]	Median CFU	*P*-value[b]
Wild-type	3.77×10^{6}		4.01×10^{5}	
Pbt^{SR}	5.17×10^{7}	0.208	2.72×10^{6}	0.068
Wild-type	2.26×10^{7}		6.29×10^{5}	
Nrp^{SR}	6.25×10^{7}	**0.045**	2.28×10^{6}	**0.036**
Wild-type	3.04×10^{7}		2.15×10^{6}	
$Nrp^{S}Pbt^{SR}$	2.70×10^{7}	0.741	3.00×10^{5}	0.106

[a] Strain defect noted as synthetase^{S} and/or receptor^{R} mutant in the proteobactin (Pbt) and/or yersiniabactin-related (Nrp) siderophore system.

[b] *P*-value determined by Mann Whitney test. Significant *P*-values are bolded.

Table 5

In vivo fitness of siderophore biosynthesis mutants following cochallenge competition experiments with *P. mirabilis* HI4320.

Strain defect[a]	Bladder		Kidneys	
	CI[b]	*P*-value[c]	CI[b]	*P*-value[c]
Pbt^{SR}	0.195	0.850	0.040	**0.034**
Nrp^{SR}	7.900	**0.004**	30.95	**0.027**
$Nrp^{S}Pbt^{SR}$	2.069	**0.019**	1.470	0.051

[a] Strain defect noted as synthetase^{S} and/or receptor^{R} mutant in the proteobactin (Pbt) and/or yersiniabactin-related (Nrp) siderophore system.

[b] Competitive index, determined by dividing the ratio of the CFU of wild-type to mutant at 7 days post-infection by the ratio present in the input inoculum. Significant CI>1 indicates mutant has a fitness defect.

[c] CI *P*-value as determined by Wilcoxon signed-rank test. Significant *P*-values are bolded.